

Supramolecular Isomerism of Coordination Compounds Based on the *in Situ* Formed $[V_2O_3]^{4+}$ Core: Discrete and Chain-like Architectures

 Mirta Rubčić,^{1,*}  Ivan Halasz,²  Gordana Pavlović,³  Damir Pajić,⁴  Edi Topić,¹  Marina Cindrić¹

¹ Department of Chemistry, Faculty of Science, University of Zagreb, Horvatovac 102a, Zagreb 10000, Croatia

² Ruđer Bošković Institute, Bijenička cesta 54, 10000 Zagreb, Croatia

³ Faculty of Textile Technology, University of Zagreb, Prilaz baruna Filipovića 28a, 10000 Zagreb, Croatia

⁴ Department of Physics, Faculty of Science, University of Zagreb, Horvatovac 102a, Zagreb 10000, Croatia

* Corresponding author's e-mail address: mirta@chem.pmf.hr

RECEIVED: March 7, 2023 * REVISED: May 18, 2023 * ACCEPTED: May 22, 2023

THIS PAPER IS DEDICATED TO PROF. BRANKO KAITNER ON THE OCCASION OF HIS 80TH BIRTHDAY

Abstract: Flexible 1,5-bis(salicylidene)carbohydrazone ligand in combination with an *in situ* formed divanadium $[V_2O_3]^{4+}$ core afforded one discrete tetranuclear complex and two polymeric chain-like architectures, mutually related as supramolecular isomers. The occurrence of a particular isomer was controlled through the reaction conditions. All isolated products were structurally characterized *via* X-ray diffraction and infrared spectroscopy, while the relative stability of the architectures was assessed *via* competitive slurry and thermal experiments. This study highlights the adaptability of oxovanadium species towards the coordination “inventory” of building blocks present in the environment, while at the same time it unveils the richness of assembly modes of the related structural units.

Keywords: vanadium(V) coordination compounds, carbohydrazone, coordination polymers.

INTRODUCTION

THE design of extended molecular systems (*e.g.* coordination polymers, organic-inorganic hybrid materials or metal-organic frameworks) as functional materials has been posed as one of the challenges for modern inorganic chemistry.^[1–5] Formation of such systems relies on coordination-driven self-assembly of building units (metal ions and/or clusters, ligands, solvent molecules and sometimes anions) often resulting in more than a single type of framework.^[6–12] While a rich assortment of ligands has been thus far utilized for their construction, attention recently focused on the flexible multitopic ones, owing to their propensity to self-adjust in response to reaction conditions and providing often unique structures.^[13–15] In this context, the carbohydrazone type of ligands have remarkable potential since they can, due to their conformational and tautomeric flexibility, accommodate metal cations in multiple coordination modes.^[16–20]

Vanadium-based metal-organic assemblies, often characterized by interesting electrical and magnetic properties, typically embrace oxovanadium clusters, whereas those containing a single cation as a node remain rare.^[21–23] This is largely due to vanadium's *in situ* adaptability, *i.e.* capability to form a variety of cores and span between oxidation states to comply with the preferences of other participants during the assembly process. Although the behaviour of vanadium may not be as predictable as is the case with *e.g.* most first transition series metal cations, such flexibility allows vanadium species to serve both as bridging moieties as well as nodes in the resulting frameworks.^[24]

Here, we demonstrate vanadium's ability to adjust towards coordination “offerings” of the multitopic carbohydrazone ligand by *in situ* formation of a divanadium core, leading altogether to three isomeric supramolecular frameworks. Each of the compounds (**1–3**) formed under specific reaction conditions, highlighting in particular the

influence of concentration and temperature on the assembly process. The compounds were thoroughly investigated in the solid state, while the relative stability of the architectures was assessed *via* competitive slurry and thermal experiments.

EXPERIMENTAL

Materials and Methods

1,5-Bis(salicylidene)carbohydrazone (H₄L) and [VO(acac)₂] were prepared according to the published literature procedures.^[25,26] Methanol was purchased from Kemika and used as received, without further purification. Elemental analyses were carried out with a Perkin-Elmer Series II 2400 CHNS/O analyser.

Infrared spectra were recorded on a PerkinElmer Spectrum RXI FTIR spectrometer from samples dispersed in KBr pellets (4000–400 cm⁻¹ range).

Thermogravimetric analyses (TGA) were performed on a Mettler-Toledo TGA/SDTA851^e thermobalance using aluminium crucibles under a nitrogen or oxygen stream with a heating rate of 5 °C min⁻¹. In all experiments the temperature ranged from 25 to 600 °C. The results were processed with the MettlerSTARe 9.01 software.

X-ray Diffraction Experiments

The general crystallographic data for **1–3** are summarized in Table 1. The data collection for **1** was conducted using Bruker D8 Advance powder diffractometer, CuKα₁ radiation from a primary Ge(111)-Johannson monochromator (for

Table 2. Crystallographic data for **1**, **2** and **3**.

	1	2	3
Chemical formula	C ₁₆ H ₁₄ N ₄ O ₇ V ₂	C ₁₈ H ₂₂ N ₄ O ₉ V ₂	C ₃₆ H ₄₄ N ₈ O ₁₈ V ₄
<i>M_r</i>	476.193	540.28	1080.55
Crystal system, colour and habit	Orthorhombic, dark green, powder	Monoclinic, red-brown, needle	Orthorhombic, red-brown, prism
Crystal dimensions (mm ³)	–	0.20 × 0.08 × 0.02	0.35 × 0.20 × 0.20
Space group	<i>Pbca</i>	<i>Cc</i>	<i>Pbca</i>
Radiation	CuKα ₁	MoKα	MoKα
<i>Z</i>	8	4	4
Unit cell parameters:			
<i>a</i> (Å)	26.236(1)	8.7792(6)	15.5137(12)
<i>b</i> (Å)	13.2390(4)	43.787(3)	13.8945(11)
<i>c</i> (Å)	10.4850(3)	5.8196(4)	20.9454(17)
α (°)	90	90	90
β (°)	90	92.899(7)	90
γ (°)	90	90	90
<i>V</i> (Å ³)	3642.3(2)	2234.3(3)	4514.9(6)
<i>T</i> (K)	293(2)	110(2)	110(2)
μ (mm ⁻¹)	–	0.894	0.88
<i>F</i> (000)	1920	1104	2208
<i>D</i> _{calc} (g cm ⁻³)	1.7370(1)	1.606	1.590
No. refined parameters, <i>N_p</i>	162	309	310
Reflections collected, unique, <i>R</i> _{int} , observed [<i>I</i> ≥ 2σ(<i>I</i>)]	–	7365, 2817, 0.064, 1911	20234, 4862, 0.044, 2830
<i>R</i> ₁ ^(a) [<i>I</i> ≥ 2σ(<i>I</i>)]/ <i>wR</i> ₂ ^(b) (all data)	<i>R_p</i> ^(c) = 0.074, <i>R_{wp}</i> = 0.110	0.040/0.0528	0.0367/0.0864
Goodness of fit on <i>F</i> ² , <i>S</i> ^(d)	1.63	0.81	0.85
Max., min. electron density (e Å ⁻³)	–	0.42, –0.34	0.29, –0.27

^(a) $R = \sum |F_o| - |F_c| / \sum |F_o|$; $w = 1 / [\sigma^2(F_o^2) + (g_1P)^2 + g_2P]$ where $P = (F_o^2 + 2F_c^2) / 3$

^(b) $wR = \{\sum [w(F_o^2 - F_c^2)^2] / \sum [w(F_o^2)^2]\}^{1/2}$

^(c) as defined in Topas

^(d) $S = \{\sum [w(F_o^2 - F_c^2)^2] / (N_r - N_p)\}^{1/2}$ where *N_r* = number of independent reflections, *N_p* = number of refined parameters.

further details see SI, Figure S1). The data collection for **2** and **3** were carried in the ω scan mode with an Oxford Xcalibur diffractometer equipped with 4-circle kappa geometry and CCD Sapphire 3 detector at 110 K. Data collection for both structures has been performed by applying the CrysAlis Software system, Version 1.171.32.24.^[27] The Lorentz-polarization effect was corrected and the intensity data was reduced by the CrysAlis RED application of the CrysAlis Software system, Version 1.171.32.24. The diffraction data have been scaled for absorption effects by the multi-scanning method. Structures were solved by direct methods and refined on F^2 by weighted full-matrix least-squares. Programs SHELXS97^[28] and SHELXL97^[28] integrated with the WinGX software system^[29] were used to solve and refine structures. All non-hydrogen atoms were refined anisotropically. Hydrogen atoms belonging to Csp^2 and Csp^3 carbon atoms were placed in geometrically idealized positions, and they were constrained to ride on their parent atoms. For compound **2**, which crystallizes in non-centrosymmetric space-group Cc , the absolute structure was assigned based on the Flack parameter, which refined to a value of $-0.02(2)$. The hydrogen atoms belonging to methanol O–H groups and amino N3 atoms were located in difference Fourier maps at the final stages of refinement and were treated with the restrained O–H and N–H distances. The molecular geometry calculations and drawings were done by PLATON^[30] and POV-Ray^[31].

Synthesis

$[V_2O_3(HL)(OCH_3)]_n$ (**1**). 1,5-Bis(salicylidene)carbohydrazone, H_4L , (0.11 g; 0.37 mmol) was added to a methanolic (20 mL) solution of $[VO(acac)_2]$ (0.20 g; 0.76 mmol). Upon addition of H_4L , the reaction mixture slowly changed colour to red-brown and was heated for 3 h. Green microcrystalline product was yielded overnight (0.10 g; 57 %). *Anal.* Calcd. mass fractions of elements, $w/\%$, for $C_{16}H_{14}N_4O_7V_2$ (476.193): C, 40.35; H, 2.96; N, 11.77; V, 21.39; found: C, 40.52; H, 3.01; N, 11.60; V, 20.48.

$\{[V_2O_3(HL)(OCH_3)] \cdot 2CH_3OH\}_n$ (**2**). The synthesis was performed similarly as for **1** but using five times smaller concentrations of reactants. H_4L (0.05 g; 0.20 mmol) and $[VO(acac)_2]$ (0.10 g; 0.38 mmol) were allowed to react in 50 mL of methanol. Red-brown needle-like product **2** (0.04 g; 39 %) deposited within several days along with small quantities of green product **1**. *Anal.* Calcd. mass fractions of elements, $w/\%$, $C_{18}H_{22}N_4O_9V_2$ (540.28): V, 18.86. Found: V, 19.27.

$[V_2O_3(HL)(OCH_3)]_2 \cdot 4CH_3OH$ (**3**). Synthesis was performed under solvothermal conditions. H_4L (0.05 g; 0.17 mmol) and $[VO(acac)_2]$ (0.10 g; 0.38 mmol) were mixed in 20 mL of methanol in a vessel which was sealed and placed in an

oven at 110 °C for 2 h. Within a few days dark brown-red prismatic crystals formed (0.05 g; 49 %). *Anal.* Calcd. mass fractions of elements, $w/\%$, $C_{18}H_{22}N_4O_9V_2$ (540.28): V, 18.86. Found: V, 18.43.

As compound **2** was air-sensitive, for the elemental analysis (except for vanadium) the product was carefully ground and left to stand for a few days in the air, allowing methanol molecules to depart. For the TGA/SDTA and IR measurements crystal were freshly harvested from the solution and analyzed. The same procedure was applied for the analysis of compound **3**. *Anal.* Calcd. mass fractions of elements, $w/\%$, for $C_{16}H_{14}N_4O_7V_2$ (476.193) (desolvated **2**): C, 40.35; H, 2.96; N, 11.77. Found: C, 40.29; H, 2.91; N, 11.62. *Anal.* Calcd. mass fractions of elements, $w/\%$, for $C_{16}H_{14}N_4O_7V_2$ (476.193) (desolvated **3**): C, 40.35; H, 2.96; N, 11.77. Found: C, 40.29; H, 2.91; N, 11.62.

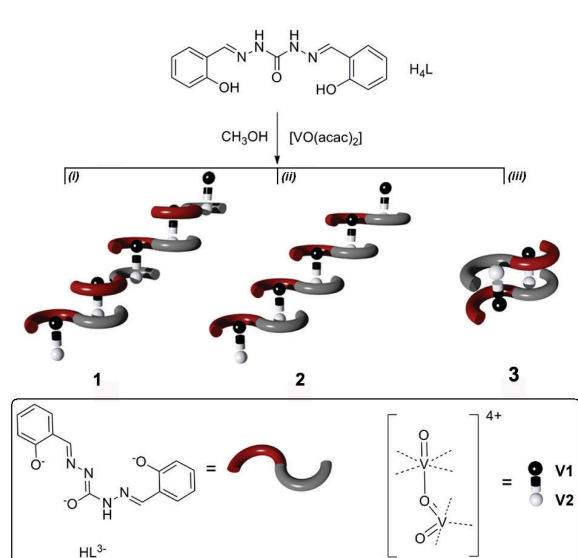
RESULTS AND DISCUSSION

The reaction of $[VO(acac)_2]$ and H_4L (Scheme 1), in relatively high concentrations (see Experimental section) in methanol and under reflux yielded exclusively a green microcrystalline product of the composition $[V_2O_3(HL)(OCH_3)]$ (**1**). If the reactant concentrations were lowered five times, alongside small quantities of **1**, a red-brown, air-sensitive, needle-like compound of the formula $[V_2O_3(HL)(OCH_3)] \cdot 2CH_3OH$ (**2**) emerged. In contrast, when the reaction was conducted under solvothermal conditions (methanol, 2 h at 110 °C), red-brown prismatic crystals (**3**), of the same composition as **2**, were harvested as the exclusive product. However, unlike **2**, crystals of **3** were air-stable for a few hours if not ground to a fine powder (Figure S2, SI).

Magnetic measurements revealed that all three compounds have negative and constant magnetic susceptibility in most of the measured temperature interval (2–240 K) (for details see SI). This clearly demonstrates the presence of only V(V) state in compounds **1–3**, which is consistent with the tendency of V(IV) species to undergo oxidation in alcoholic solutions.^[32,33]

Structural analysis via powder X-ray diffraction (PXRD) for **1** (Figure S1, SI), and single crystal X-ray diffraction (SCXRD) for **2** and **3** revealed that, not considering the solvate molecules, architectures of the three isomers are assembled from the same building blocks: the deprotonated ligand (HL^{3-}), in situ formed oxodivanadium core, and the methoxo group as a capping ligand (Scheme 1 and Figure 1).

A one-dimensional chain-like architecture is found in compounds **1** and **2** (Figure 1(a) and (b), Table S1), while **3** assumes a discrete square tetranuclear structure (Figure 1(c), Table S1). In all three architectures, the deprotonated



Scheme 1. Reaction path and schematic representation of chains and a discrete square architecture forms for compounds **1**, **2** and **3**. Each compound was obtained under specific reaction conditions: (i) **1** (reflux, ambient pressure); (ii) **2** (reflux, ambient pressure, reaction mixture five times more diluted than (i)); (iii) **3** (solothermal conditions, 2 h at 110 °C). Stepwise chain architectures (**1** and **2**) form if the neighbouring $[V_2O_3]^{4+}$ units have the same orientation. If the neighbouring $[V_2O_3]^{4+}$ units have the opposite orientation discrete square architecture forms, **3**. Dashed lines in the representation of the $[V_2O_3]^{4+}$ core designate vacant coordination sites. The capping methoxy moiety, which is omitted for clarity, occupies one of the V1 coordination sites.

ligand (HL^{3-}) assumes an anti-conformation, which is realized through the flip around the central C–N linkage (Scheme 1). Such conformational rearrangement provides two non-equivalent coordination pockets which accommodate vanadium atoms of two $[V_2O_3]^{4+}$ cores in a dianionic O,N,O (V1) and in a monoanionic N,N,O fashion (V2) (Figure S3, SI). On the other hand, each $[V_2O_3]^{4+}$ unit, acting as a secondary building unit, provides two sets of vacant coordination sites; nearly square-planar around the V1 atom and T-shaped around the V2 atom (Scheme 1). Finally, methoxy moiety binds to the V1 atom completing its distorted octahedral coordination environment. In contrast, the V2 atom remains in a distorted tetragonal-pyramidal coordination environment.

The $[V_2O_3]^{n+}$ core ($n = 2, 3, 4$) is not uncommon in vanadium coordination chemistry (Table S2 and Figure S4).^[32] However, complexes with asymmetric coordination environments are not so numerous, with few known examples where vanadium ions assume, as is the

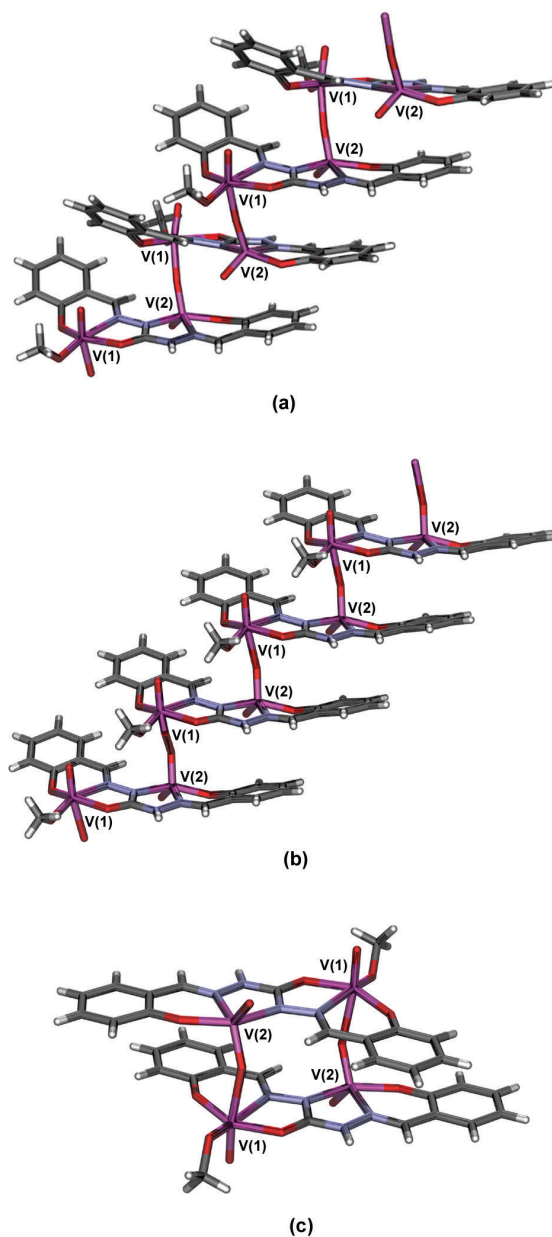


Figure 1. Mercury POV-Ray rendered view of the architectures found in: (a) **1**, (b) **2**, and (c) **3**. Stepwise chains are found in: (a) **1** and (b) **2**. In both architectures, the neighboring $[V_2O_3]^{4+}$ units have the same orientation ($V_2 \rightarrow V_1$ direction). In **1** neighboring ligands are arranged in a head-to-tail manner, while in **2** they are arranged in a head-to-head fashion. (c) The discrete square architecture of compound **3**. The two neighbouring $[V_2O_3]^{4+}$ units are orientated oppositely ($V_2 \rightarrow V_1$ direction). In (b) and (c) solvate methanol molecules are omitted for clarity. In **1**, $[V_2O_3]^{4+}$ cores have twist-angular configuration, while in **2** and **3** the cores assume anti-angular configuration (for detailed description see Table S1 and Figure S4 in the SI).

case here, different coordination geometries.^[20,34–38] Such systems have stimulated considerable attention since they can be considered as models for the construction of heterometallic complexes. It should be noted that a solvate of the tetranuclear complex **3** has been previously reported.^[20] However, compounds **1** and **2** presented here are the rare examples of the $[V_2O_3]^{4+}$ core-based systems with nuclearity greater than four.

Thus, starting from the same building units, architectures of compounds **1** to **3** are realized through different orientations of the neighbouring $[V_2O_3]^{4+}$ cores. The same orientation of adjacent divanadium units ($V_2 \rightarrow V_1$ direction; Figure 1(a) and Figure 1(b)) gives rise to stepwise chains, found in compounds **1** and **2**. On the contrary, when the adjacent $[V_2O_3]^{4+}$ units run in the opposite direction a discrete square architecture is realized (Figure 1(c)). Underlying architectures of **1** and **2** differ in relative arrangements of ligands within chains. While in **1** the two neighbouring ligands assume a head-to-tail arrangement (Figure 1(a)), in chains of **2** they are arranged in a head-to-head manner (Figure 1(b)). It is also worth noting that the repeating $[V_2O_3(HL)(OCH_3)]$ fragments found in architectures of **1–3** differ substantially in their conformations (Figure 2). Given that the underlying architectures of **1–3**, not considering the solvate methanol molecules, arise from different assembly modes of identical building units, they can be best classified as structural supramolecular isomers.^[7]

When comparing infra-red (IR) spectra of **2** and **3** with the spectrum of **1**, the biggest differences are attributed to the presence of solvate methanol molecules and different hydrogen bonding patterns (Figure S5–S7, Table S3, SI). In the spectrum of **1**, a band due to NH stretching is clearly visible at 3245 cm^{-1} (Figure S8, SI). Although overlapped with a broad band centred at $\sim 3400\text{ cm}^{-1}$ arising from methanol O–H stretching, in spectra of **2** and **3** this band is found at 3230 cm^{-1} and 3229 cm^{-1} , respectively (Figure S8, SI). A band due to C–O stretching of the coordinated methoxo group appears as a sharp singlet at 1035 cm^{-1} in the spectrum of **1**. In contrast, spectra of **2** and **3** exhibit additional maxima around 1040 cm^{-1} corresponding to C–O stretching of the solvate methanol molecules (SI). In the region below 1000 cm^{-1} bands of terminal V=O stretching appear at 954 cm^{-1} and 918 cm^{-1} for **1**, 956 and 918 cm^{-1} for **2**, and 954 cm^{-1} , 920 cm^{-1} for **3**. Bands of the antisymmetric V–O–V bridge vibration are, for all three compounds, observed around 840 cm^{-1} (SI). The spectrum of **1** shows a greater resemblance to that of **2**, especially in the region below 1000 cm^{-1} , which is indicative of their similar underlying architectures (Figure S8(d), SI).

TGA/SDTA analyses revealed similar and complicated multi-step decomposition patterns for **1–3**

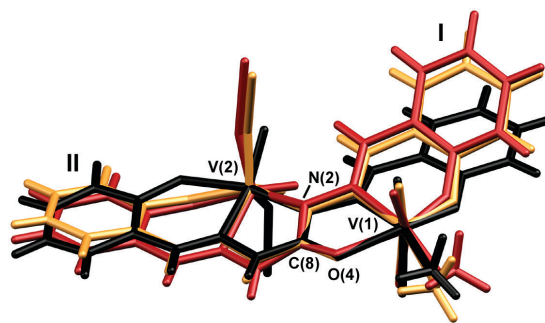


Figure 2. Mercury POV-Ray rendered view of overlapping diagrams for: **1** (red), **2** (orange) and **3** (black). Diagrams were constructed by overlapping molecules through V(1), O(4), C(8), N(2) and V(2) atoms. Dihedral angles between the planes I and II of the salicylidene rings (I–plane through atoms C(1)–C(6) and II–plane through atoms C(10)–C(15), see SI) are: $45.91(6)^\circ$ (for **1**), $34.0(3)^\circ$ (for **2**), $4.65(12)^\circ$ (for **3**).

(Figure S9, SI). Compound **1** exhibits the highest thermal stability up to $\approx 220\text{ }^\circ\text{C}$. For compounds **2** and **3**, the weight losses up to $\approx 150\text{ }^\circ\text{C}$ are due to the loss of solvate methanol, while degradation of the underlying frameworks commences around $200\text{ }^\circ\text{C}$ for **2** and around $170\text{ }^\circ\text{C}$ for **3**. Compound **3** is stable up to $\approx 50\text{ }^\circ\text{C}$ after which solvent molecules are lost in two steps. On the other hand, **2** loses methanol almost immediately upon removal from the solution. Such a difference reflects the difference in bonding of methanol molecules in their crystal structures (Figure S6 and Figure S7, SI). Finally, it should be noted that transformation(s) among frameworks were not observed upon heating.

Since there is a certain analogy between polymorphism and supramolecular isomerism, attempts were made to transform and evaluate the stability of the prepared architectures via recrystallization and slurry experiments. These were conducted in methanol, due to the potential exchange of the alkoxo ligand in higher alcohols.^[32] Competitive slurry revealed that conversion among frameworks does not occur at room temperature, even after 72 hours. In contrast, when the experiment was performed in boiling methanol, after 8 hours the only remaining product was **1** (Figure S10, SI), rendering its architecture as the most stable at a given temperature.

CONCLUSION

We have demonstrated that metal cations with the ability to form oxoclusters *in situ* in combination with flexible ligands offer a spectrum of possibilities for the synthesis of extended coordination systems. Responding to the

asymmetric chelating characteristics of the carbohydrazone ligand, vanadium adopts a specific core and based upon the reaction conditions, control was achieved over formation among three isomeric frameworks of different dimensionalities. Further investigations will be focused on the possible extension of dimensionality to two- and three-dimensional architectures through the replacement of the capping ligands.

Acknowledgements. We are thankful to Ms Ljubica Ljubić for the help with synthetic procedures.

Conflict of Interest. The authors declare no potential conflicts of interest.

Supplementary Materials. Supplementary materials contain details of powder diffraction analysis, magnetic measurements, molecular and crystal structures, IR spectroscopy and thermal analyses are attached to the electronic version of the article at: <https://doi.org/10.5562/cca3995>.

Supplementary crystallographic data sets for the structures **1**, **2** and **3** are available through the Cambridge Structural Data base with deposition numbers 2260574–2260576. Copies of this information may be obtained free of charge from the director, CCDC, 12 Union Road, Cambridge, CB2 1EZ, UK (fax: +44 1223 336 033; E-mail: deposit@ccdc.cam.ac.uk or at <http://www.ccdc.cam.ac.uk>).

PDF files with attached documents are best viewed with Adobe Acrobat Reader which is free and can be downloaded from Adobe's web site.

REFERENCES

- [1] S. Kitagawa, R. Kitaura, S. Noro, *Angew. Chem. Int. Ed.* **2004**, 43, 2334–2375. <https://doi.org/10.1002/anie.200300610>
- [2] J. L. C. Rowsell, O. M. Yaghi, *Angew. Chem. Int. Ed.* **2005**, 44, 4670–4679. <https://doi.org/10.1002/anie.200462786>
- [3] J. J. Perry IV, J. A. Permana, M. J. Zaworotko, *Chem. Soc. Rev.* **2009**, 38, 1400–1417. <https://doi.org/10.1039/b807086p>
- [4] G. H. Morritt, H. Michaels, M. Freitag, *Chem. Phys. Rev.* **2022**, 3, 011306. <https://doi.org/10.1063/5.0075283>
- [5] G. Férey, *Chem. Soc. Rev.* **2008**, 37, 191–214. <https://doi.org/10.1039/B618320B>
- [6] S. R. Batten, S. M. Neville, D. R. Turner, *Coordination Polymers, Design, Analysis and Application*, RSC, Cambridge, **2009**.
- [7] J.-P. Zhang, X.-C. Huang, X.-M. Chen, *Chem. Soc. Rev.* **2009**, 38, 2385–2396. <https://doi.org/10.1039/b900317g>
- [8] O. M. Yaghi, M. O'Keeffe, N. W. Ockwig, H. K. Chae, M. Eddaoudi, J. Kim, *Nature* **2003**, 423, 705–714. <https://doi.org/10.1038/nature01650>
- [9] H. Abourahma, B. Moulton, V. Kravtsov, M. J. Zaworotko, *J. Am. Chem. Soc.* **2002**, 124, 9990–9991. <https://doi.org/10.1021/ja027371v>
- [10] S. A. Barnett, A. J. Blake, N. R. Champness, C. Wilson, *Chem. Commun.* **2002**, 15, 1640–1641. <https://doi.org/10.1039/b203661d>
- [11] V. Vrdoljak, B. Prugovečki, D. Matković-Čalogović, R. Dreos, P. Siega, C. Tavagnacco, *Cryst. Growth Des.* **2010**, 10, 1373–1382. <https://doi.org/10.1021/cg901382h>
- [12] T. D. Hamilton, G. S. Papaefstathiou, T. Friščić, D.-K. Bučar, L. R. MacGillivray, *J. Am. Chem. Soc.* **2008**, 130, 14366–14367. <https://doi.org/10.1021/ja804863u>
- [13] A. J. Blake, N. R. Brooks, N. R. Champness, M. Crew, A. Deveson, D. Fenske, D. H. Gregory, L. R. Hanton, P. Hubberstey, M. Schröder, *Chem. Commun.* **2001**, 16, 1432–1433. <https://doi.org/10.1039/b103612m>
- [14] T. L. Hennigar, D. C. MacQuarrie, P. Losier, R. D. Rogers, M. J. Zaworotko, *Angew. Chem. Int. Ed. Engl.* **1997**, 36, 972–973. <https://doi.org/10.1002/anie.199709721>
- [15] M. du Plessis, L. J. Barbour, *Dalton Trans.* **2012**, 41, 3895–3898. <https://doi.org/10.1039/C1DT11564B>
- [16] C. Bustos, O. Burckhardt, R. Schreiber, D. Carrillo, A. M. Arif, A. H. Cowley, C. M. Nunn, *Inorg. Chem.* **1990**, 29, 3996–4001.
- [17] V. A. Kogan, V. V. Lukov, V. M. Novotortsev, I. L. Eremenko, G. G. Aleksandrov, *Russ. Chem. Bull. Int. Ed.* **2005**, 54, 600–605. <https://doi.org/10.1007/s11172-005-0294-4>
- [18] E. Topić, J. Pisk, D. Agustin, M. Jendrlin, D. Cvijanović, V. Vrdoljak, M. Rubčić, *New J. Chem.* **2020**, 44, 8085–8097. <https://doi.org/10.1039/D0NJ01045F>
- [19] E. Topić, I. Landripet, M. Duguin, J. Pisk, I. Đilović, V. Vrdoljak, M. Rubčić, *New J. Chem.* **2020**, 44, 13357. <https://doi.org/10.1039/D0NJ03106B>
- [20] D. Dragancea, N. Talmaci, S. Shova, G. Novitchi, D. Darvasiová, P. Rapta, M. Breza, M. Sophia Galanski, J. Kožíšek, N. M. R. Martins, L. M. D. R. S. Martins, A. J. L. Pombeiro, V. B. Arion, *Inorg. Chem.* **2016**, 55, 9187. <https://doi.org/10.1021/acs.inorgchem.6b01011>
- [21] M. Yuan, E. Wang, Y. Lu, S. Wang, Y. Li, L. Wang, C. Hu, *Inorganica Chim. Acta* **2003**, 344, 257–261. [https://doi.org/10.1016/S0020-1693\(02\)01260-4](https://doi.org/10.1016/S0020-1693(02)01260-4)
- [22] Z.-F. Chen, H. Liang, H.-M. Hu, Y. Li, R.-G. Xiong, X.-Z. You, *Inorg. Chem. Comm.* **2003**, 6, 241–243. [https://doi.org/10.1016/S1387-7003\(02\)00736-0](https://doi.org/10.1016/S1387-7003(02)00736-0)
- [23] X.-M. Zhang, M.-L. Tong, H. Kay Lee, X.-M. Chen, *J. Solid State Chem.* **2001**, 160, 118–122. <https://doi.org/10.1006/jssc.2001.9202>
- [24] J. Zhu, X. Chen, A. Q. Thang, F.-L. Li, D. Chen, H. Geng, X. Rui, Q. Yan, *SmartMat.* **2022**, 3, 384–416. <https://doi.org/10.1002/smm2.1091>

- [25] M. Rubčić, N. Galić, I. Halasz, T. Jednačak, N. Judaš, J. Plavec, P. Šket, P. Novak, *Cryst. Growth Des.* **2014**, *14*, 2900–2912. <https://doi.org/10.1021/cg500203k>
- [26] R. A. Rowe, M. M. Jones, in *Inorganic Synthesis – vol. V*. (Ed.: T. Moeller) McGraw-Hill Book Company, Inc: New York, **1957**, pp. 113–116.
- [27] Oxford Diffraction Ltd., Xcalibur CCD system, CrysAlis Software system, Versions 1.171.32.24. Abingdon, Oxfordshire, England, **2008**.
- [28] G. M. Sheldrick, *Acta Cryst.* **2008**, *A64*, 112–122. <https://doi.org/10.1107/S0108767307043930>
- [29] L. J. Farrugia, *J. Appl. Cryst.* **1999**, *32*, 837–838. <https://doi.org/10.1107/S0021889899006020>
- [30] A. L. Spek, *J. Appl. Cryst.* **2003**, *36*, 7–13. <https://doi.org/10.1107/S0021889802022112>
- [31] <https://www.povray.org/>
- [32] M. Rubčić, D. Milić, G. Horvat, I. Đilović, N. Galić, V. Tomišić, M. Cindrić, *Dalton Trans.* **2009**, 9914–9923. <https://doi.org/10.1039/b913653c>
- [33] M. Rubčić, D. Milić, G. Pavlović, M. Cindrić, *Cryst. Growth Des.* **2011**, *11*, 5227–5240. <https://doi.org/10.1021/cg200466b>
- [34] C. Drouza, A. D. Keramidias, *J. Inorg. Biochem.* **2000**, *80*, 75–80. [https://doi.org/10.1016/S0162-0134\(00\)00042-8](https://doi.org/10.1016/S0162-0134(00)00042-8)
- [35] A. Neves, L. M. Rossi, A. J. Bortoluzzi, A. S. Mangrich, W. Haase, O. R. Nascimento, *Inorg. Chem. Comm.* **2002**, *5*, 418–421. [https://doi.org/10.1016/S1387-7003\(02\)00436-7](https://doi.org/10.1016/S1387-7003(02)00436-7)
- [36] A. Sarkar, S. Pal, *Eur. J. Inorg. Chem.* **2009**, 5391–5398. <https://doi.org/10.1002/ejic.200900680>
- [37] P. B. Chatterjee, N. Kundu, S. Bhattacharya, Ki-Young Choi, A. Endo, M. Chaudhury, *Inorg. Chem.* **2007**, *46*, 5483–5485. <https://doi.org/10.1021/ic700858g>
- [38] P. B. Chatterjee, N. Kundu, S. Bhattacharya, Ki-Young Choi, A. Endo, M. Chaudhury, *Inorg. Chem.* **2008**, *47*, 4891–4902. <https://doi.org/10.1021/ic800208w>